Quantum transport of buried single-crystalline $CoSi_2$ layers in (111)Si and (100)Si substrates

Klaus Radermacher
Institut für Schicht- und Ionentechnik, Forschungszentrum Jülich, D-52425 Jülich, Germany

Don Monroe, Alice E. White, and Ken T. Short
AT&T Bell Laboratories, 600 Mountain Avenue, Murray Hill, New Jersey 07974

Rolf Jebasinski
Institut für Schicht- und Ionentechnik, Forschungszentrum Jülich, D-52425 Jülich, Germany
(Received 29 December 1992)

Magnetoresistance data for clean crystalline $CoSi_2$ layers were analyzed in terms of weak localization, Coulomb interactions, and superconducting fluctuations. The $CoSi_2$ layers with thicknesses of 11.5 nm in (111)Si and 23 nm in (100)Si were fabricated by high-dose ion implantation and subsequent annealing in a rapid thermal annealer (known as ion-beam synthesis or mesotaxy). The magnetic-field dependence of the resistance is interpreted in terms of two-dimensional weak localization with strong spin-orbit interaction and an addtional classical contribution proportional to H^2. No indication of magnetic scattering was found, which is a sign of the "cleanness" of the samples. Long phase-coherence lengths of $l_\phi \approx 0.75$ μm in (111)Si and $l_\phi \approx 2.3$ μm in (100)Si at 4.2 K were determined by fitting the magnetoresistance data. The inferred inelastic-scattering time is interpreted as a sum of a clean-limit electron-electron process (dominant at temperatures below ≈ 6 K) and an electron-phonon process dominant at higher temperatures. We further observed a general orientation dependence of the electrical transport properties of mesotaxial $CoSi_2$ layers, such as anisotropy in the residual resistance, Hall coefficient, and the prefactor for the classical H^2 dependence of the magnetoresistance. This is probably related to multiple-band effects in $CoSi_2$.

I. INTRODUCTION

The controlled formation of epitaxial silicides on silicon is of great interest for application in silicon integrated circuits,[1] as well as for fundamental research. The metallic disilicides $NiSi_2$ and $CoSi_2$ are unique among silicides, since they have a cubic fluorite structure similar to the diamond structure of Si with a lattice mismatch to Si at room temperature for $CoSi_2 = -1.2\%$ and $NiSi_2 = -0.46\%$. These properties are favorable for the formation of epitaxial silicide layers with atomically sharp interfaces to the Si substrates. Thus these silicides are candidates for the fabrication of microstructure devices in which quantum interference effects play essential roles both for the fundamental study of quantum size effects and Anderson localization. For an overview of quantum effects in metals, see Ref. 2. Possible device applications are included in Ref. 3.

Electrical transport properties of epitaxial $NiSi_2$ and $CoSi_2$ layers have been reported by several authors. Hensel *et al.* showed that the resistivity of UHV-deposited $CoSi_2$ layers is independent of thickness down to 10 nm.[4] From the residual resistance, they obtained a mean free path l_0 of about 100 nm, showing that the scattering of conduction electrons is essentially specular. In addition, they attributed the strong divergence of the residual resistivity as a function of the inverse layer thickness for very thin layers (< 10 nm) due to quantum size effects.[5,6]

Many experiments on weak localization in "dirty" metals (where $k_F l_0 < 1$) have been reported,[7] but few have been reported on single-crystalline metals ("clean" metals $k_F l_0 \gg 1$). Matsui *et al.*[8] measured the phase-coherent length l_ϕ of conduction electrons in single-crystal $NiSi_2$ by using weak-localization phenomena. From these measurements they deduced $l_\phi = 0.8$ μm at 4.2 K and 1.5 μm at 2 K. These long phase-coherent lengths are due to the good crystallinity and the low concentration of impurities in their samples. For ultrathin $CoSi_2$ films fabricated with solid phase epitaxy, DiTusa, Parpia, and Phillips[9] measured a temperature-independent contribution to the phase breaking scattering rate and attributed this to spin-spin scattering of the conduction electrons, which increases as the thickness is decreased. This magnetic scattering was not attributed to a random distribution of magnetic impurities but rather to magnetic defects at the Si/$CoSi_2$ interface which are believed to be magnetic cobalt atoms. For $CoSi_2$ layers with thicknesses lower than 10 nm, Badoz *et al.*[10] found that the superconducting critical temperature T_C was abruptly depressed, and also attributed this to the presence of magnetic impurities of "ill-coordinated" cobalt atoms at the interface. In contrast, in well-annealed films grown by a codeposition technique, von Känel[11] found a temperature dependence of the phase breaking time τ_ϕ of approximately $\tau_\phi \propto T^{-1}$ in a temperature range from 2.8 to 10 K, indicating no dominant magnetic scattering. Thus the presence of magnetic scattering is a property of the interface coordination, which depends on the preparation technique, and

0163-1829/93/48(11)/8002(14)/$06.00

is not an intrinsic property of $CoSi_2$. For this reason, we fabricated "mesotaxial" thin buried $CoSi_2$ layers in (111)Si and (100)Si by high-dose Co^+ implantations in single-crystal Si substrates and subsequent high-temperature annealing.[12,13] This technique has several advantages: due to mass selective implantation, the layers show a very high purity; and, due to annealing at temperatures above 1000 °C, the Co atoms at the interfaces are apparently well coordinated. A further advantage is the existence of a single-crystal Si top layer which can be used as a seed for further Si epitaxy. In addition, *in situ* patterning of $CoSi_2$ layers is possible by implantation through a mask. Wires down to 0.25-μm width have been fabricated by this technique.[14] Since the elastic-scattering length of the charge carrier in $CoSi_2$ is long compared with that in $NiSi_2$, we expect a longer phase-coherence length. These properties (large elastic-scattering time and good layer quality due to mesotaxial fabrication technique) are advantageous for exploring quantum interference effects in single-crystalline $CoSi_2$ structures.

II. EXPERIMENT

Co^+ implantation into high-resistivity silicon wafers ($\rho > 2000\,\Omega$ cm) at elevated temperatures was performed with a medium current ion accelerator (EATON NV-3204). The temperature was measured by a thermocouple in the heated substrate holder. The crystal quality and also the electrical properties of thin $CoSi_2$ layers are very sensitive to the fabrication parameters.[15] In (111)Si, 11.5-nm-thick $CoSi_2$ layers were fabricated by 20-keV implantation of 3.5×10^{16} Co^+ cm^{-2} at a substrate temperature of 425 °C (current density ≈ 1.3 μA cm^{-2}) and subsequent rapid thermal annealing (RTA) at 750 °C for 10 s and 1150 °C for 10 s. These layers have very sharp interfaces and high crystal quality (minimum yield value of about 4% in the Co signal). In (100)Si, the fabrication of thin layers is even more complicated. A continuous $CoSi_2$ layer is formed by 40-keV implantion, with a dose of 6.5×10^{16} Co^+ cm^{-2} at a substrate temperature of 425 °C (current density ≈ 4.5 μA cm^{-2}) and subsequent RTA at 1100 °C for 5 s. As confirmed by transmission electron microscopy, this layer is continuous with a thickness of 23 nm and sharp interfaces to the Si substrate. Only occasional steps with $\{111\}$ facets, typical of (100)-oriented samples,[15] are observed. These buried $CoSi_2$ layers were subsequently patterned in a 50-μm-wide mesa structure with eight contact pads, each 600 μm apart. At the contact pads the top silicon was removed, Cr/Au was evaporated for ohmic contacts, and all samples were subsequent inserted into a chip carrier.

The samples were mounted in a ^{3}He cryostat. Four probe resistance measurements of the layers and the wires as a function of temperature and magnetic field were performed using an ac Wheatstone-type bridge at a frequency of 1 kHz. The resistance and Hall measurements were performed with currents of 10–100 μA. A comparison of resistivity measurements in the dependence of the magnetic field at 1.2 K shows no difference in the data measured at 10 or 100 μA. This is an indication that heating of the samples or hot-electron effects are negligible. In order to obtain a higher signal-to-noise ratio, we performed all measurements at a current of 100 μA.

III. THEORETICAL BACKGROUND

Since the calculated mean free paths l_0 of the layers (from residual resistance measurements, see Sec. IV A) are larger than the thickness of the $CoSi_2$ films, the layers are fully two dimensional with respect to the normal conduction process. Also, the factor $k_F l_0 \gg 1$ (k_F= Fermi wave vector $=9.1\times10^7$ cm^{-1}, see Table I in Sec. IV A), indicating that two dimensional (2D) theories of quantum transport in the case of a "clean" metal can be successfully applied to both samples. As pointed out by Bergmann,[16] the analysis of magnetoresistance in the presence of superconducting fluctuations above the critical temperature T_C is very difficult, since the quantum corrections to the resistivity are composed of several terms. These corrections to the classical Drude resistance at low temperatures are (i) the classical magnetoresistance; (ii) weak localization; (iii) Maki-Thompson (MT) superconducting fluctuations; (iv) Aslamazov-Larkin (AL) superconducting fluctuations; (v) the Coulomb contribution to the particle-hole channel (CPH); (vi) the Coulomb interaction in the particle-particle channel (CPP); and (vii) electron-phonon scattering. Unfortunately, all these contributions can act simultaneously, and the question now arises as to which of these effects are really important in $CoSi_2$. For this reason we will first briefly discuss the different contributions theoretically, and compare these predictions with our experimental data in Sec. IV. To compare with the experiment, we will focus on the lower-order magnetoresistance $\propto H^2$. We express the coefficient as where $\Delta R/R_0^2=\gamma(T)\xi H^2$ [with $\xi=e^2/(\pi h)\approx 1.233\times10^{-5}$ Ω^{-1} (h is the Planck's constant, e the electron charge)].

A. Classical magnetoresistance in metals

Classical magnetoresistance is observed in metals with several partially filled conduction bands.[17] In lowest order, the normalized magnetoresistance is given by the equation

$$\frac{\rho(H)-\rho(H=0)}{\rho(H=0)}=\omega_c^2\tau_0^2=\alpha_1 H^2 , \qquad (1)$$

where $\omega_C=eH/m^*$ (m^* is the effective mass). By measuring the prefactor α_1, the elastic-scattering time τ_0 can be estimated. Since band-structure calculations[18] show that three-hole bands contribute to the electrical transport in $CoSi_2$, a classical contribution to the magnetoresistance is expected.

B. Localization in 2D systems

The fractional change in the resistance due to weak localization at a given temperature and magnetic field was first calculated by Altshuler *et al.*[19] Hikami, Larkin, and Nagaoka[20] and Maekawa and Fukuyama[21] include spin-orbit and magnetic scattering in their analysis of quantum interference:

$$\frac{\Delta R}{R_0^2}=\xi\left[\psi\left[\frac{1}{2}+\frac{H_1}{H}\right]-\frac{3}{2}\psi\left[\frac{1}{2}+\frac{H_2}{H}\right]+\frac{1}{2}\psi\left[\frac{1}{2}+\frac{H_3}{H}\right]-\ln\left[\frac{H_1H_3^{1/2}}{H_2^{3/2}}\right]\right] \tag{2a}$$

where $\Delta R=R(H)-R(H=0)$ is the change in resistance, $R_0=R(H=0)$ is the resistance without magnetic field, H is the magnetic field, and the H_n's are defined as follows:

$$\begin{aligned} H_1&=H_0+H_{\text{s.o.}}+H_s\ , \\ H_2&=\tfrac{4}{3}H_{\text{s.o.}}+\tfrac{2}{3}H_s+H_{\text{in}}\ , \\ H_3&=2H_s+H_{\text{in}}\ , \end{aligned} \tag{2b}$$

with $H_n\tau_n=h/(8\pi eD)$. In these equations H_0 corresponds to the elastic lifetime τ_0, H_{in} to the inelastic lifetime τ_{in}, $H_{\text{s.o.}}$ to the spin-orbit scattering time $\tau_{\text{s.o.}}$, and H_S to the magnetic scattering ring time τ_s. ψ is the digamma function and D the diffusion constant: $D=v_Fl_0/z$, where z is the dimension of the system (in our case, $z=2$), l_0 the elastic mean free path of the charge carrier, and v_F the Fermi velocity. Bergmann calculated the magnetoresistance to lower order in the magnetic field:[16]

$$\frac{\Delta R}{R_0^2}\approx\xi\tfrac{1}{24}\left[\frac{1}{H_1^2}-\frac{3}{2}\frac{1}{H_2^2}-\frac{1}{2}\frac{1}{H_3^2}\right]\mathrm{H}^2=\gamma_L(T)\xi\mathrm{H}^2\ . \tag{3}$$

C. Maki-Thompson contribution

Since our films are in the two-dimensional limit, we have to use the 2D expression for this contribution. The physical interpretation was given by Larkin.[22] An electron at the Fermi surface experiences inelastic-scattering processes and, after an inelastic lifetime τ_{in}, the electron is scattered into a new energy eigenstate. If one of the electrons is now a partner of a virtual Cooper pair (above T_C), the Cooper pair is broken. Larkin showed that these superconducting fluctuations contribute to the resistivity corresponding to the Maki-Thompson diagram, and that the magnetic-field dependence of the resistance is the same as for weak localization, but with a coefficient $\beta(T)$ which diverges at T_C:

$$\frac{\Delta R}{R_0^2}=\xi\beta(T)\left[\psi\left[\frac{1}{2}+\frac{H_{\text{in}}}{H}\right]+\ln\left[\frac{H}{H_{\text{in}}}\right]\right]\ . \tag{4}$$

$\beta(T)$ is defined and tabulated by Larkin:[22] $\beta(T)\approx\pi^2/4(\ln(T/T_C))^{-1}$ in the vicinity of T_C, and $\beta(T)=\pi^2/6(\ln(T/T_C))^{-2}$ at a temperature well above T_C. H_{in} can be determined in magnetoresistance measurements (see Sec. III C). However, there are some restrictions on the validity of Larkin's theory:

$$\ln\left[\frac{T}{T_c}\right]\gg\frac{h}{4\pi^2k_BT\tau_{\text{in}}}\ , \tag{5a}$$

$$4DeH\ll k_BT\ln\left[\frac{T}{T_c}\right]\ . \tag{5b}$$

In low magnetic fields, the magnetoresistance is given by[22]

$$\frac{\Delta R}{R_0^2}\approx\frac{\beta(T)}{24}\xi\mathrm{H}^2=\gamma_{\mathrm{MT}}(T)\xi\mathrm{H}^2\ . \tag{6}$$

For the temperature dependence in zero magnetic field, Altshuler *et al.*[23] calculated the following expression, which is due to the fact that the cutoff energy in the calculation of the MT term is $k_BT\ln(T/T_C)$:

$$\frac{\Delta R}{R_0^2}=\xi\beta(T)\ln\left[\frac{\ln\left[\frac{T}{T_C}\right]}{\delta}\right]\ , \tag{7}$$

where $\delta=h(16k_BT\tau_{\text{in}})^{-1}$ is the Maki-Thompson pair-breaking parameter. Restrictions (5a) and (5b) limit the calculation to low magnetic fields. It was argued[24] that $\beta(T)$ may be depressed in magnetic fields comparable to the upper critical magnetic field, H_{C_2}, and deviations from Larkin's theory can be accounted for by proposing a field-dependent $\beta(T,H)$.[25] However, at large fields, the theoretical curves differ from the experimental data, e.g., as found for Al films.[26] Lopes dos Santos and Abrahams[27] extended the Maki-Thompson results closer to T_C and to higher magnetic fields by considering the magnetic-field dependence of the superconducting fluctuations. In zero magnetic field, they obtained

$$\left[\frac{\Delta R}{R_0^2}\right]_{\mathrm{MT}}(T,H=0)=\frac{\pi^2}{4}\xi\frac{1}{\ln\left[\frac{T}{T_c}\right]-\delta}\ln\left[\frac{\ln\left[\frac{T}{T_c}\right]}{\delta}\right]\ . \tag{8}$$

The theory in Ref. 27 predicts a saturation of the magnetoresistance at a value which is $-(\Delta R/R_0^2)_{\mathrm{MT}}(H=0)$. This reflects the fact that the magnetic field quenches the superconducting fluctuations and completely suppresses the extra conductance due to the MT diagram. But to our knowledge, there is not yet a theoretical description of Maki-Thompson fluctuations for all temperatures over a large range of magnetic fields.

D. Aslamazov-Larkin contribution

Aslamazov and Larkin[28] calculated the influence of superconducting fluctuations in two-dimensional disordered superconductors on the resistance above the critical temperature. The variations of this contribution in a perpendicular magnetic field was first derived by Usadel,[29] and is also found to be proportional to H^2 to lowest order:[16]

$$\frac{\Delta R}{R_0^2}=-\frac{\pi^2}{16}\xi\frac{1}{\left[\ln\left[\frac{T}{T_c}\right]\right]^3}\frac{1}{\left[T\frac{dH_{C_2}}{dT}\right]^2}\mathrm{H}^2=\gamma_{\mathrm{AL}}(T)\xi\mathrm{H}^2, \tag{9}$$

where dH_{C_2}/dT is the derivative of the upper critical field. As seen from Eq. (9), the Aslamazov-Larkin contribution is determined by the critical temperature T_C and the slope of the upper critical field H_{C_2}.

E. Coulomb interaction

Altshuler, Aronov, and Lee[30] and Fukuyama[31] found that the contribution of Coulomb interaction to the resistivity is independent of the magnetic field. However, Lee and Ramakrishnan[32] calculated a positive magnetoresistance in the particle-hole channel due to the effect of the field on the spins of the electrons:

$$\frac{\Delta R}{R_0^2} \approx \begin{cases} \xi \frac{F}{2} 0.084\eta^2 \ , & \eta \ll 1 \\ \xi \frac{F}{2} \ln\left[\frac{\eta}{1.3}\right] \ , & \eta \gg 1 \ , \end{cases} \tag{10}$$

where $\eta = g\mu_B H/(k_B T)$, g is the g factor, and μ_B the Bohr magneton. F is a parameter representing the degree of screening of the Coulomb interaction, and varies between $F=0$ for complete screening and $F=1$ for bare interaction. Typical values of F for thin metal films are on the order of 0.2–0.25.[33] This value can be reduced in the presence of spin-orbit scattering, but we can use these values to estimate the contribution of spin-orbit scattering to the magnetoresistance of $CoSi_2$ layers.

For the Kubo graph of Coulomb interaction with particle-particle propagator, Altshuler *et al.*[24] calculated the magnetoresistance. For low magnetic fields, the magnetoresistance is again proportional to H^2 (Ref. 24):

$$\frac{\Delta R}{R_0^2} = \xi \frac{1}{\ln\left[\frac{T}{T_c}\right]} \left[\frac{\zeta(3)}{4}\right] \frac{1}{H_T^2} \mathrm{H}^2 = \gamma_{\mathrm{cpp}}(T)\xi H^2 \ , \tag{11}$$

with $H_T = \pi k_B T/(2eD)$ and $\zeta(3)$ is the Rieman ζ function.

IV. EXPERIMENTAL RESULTS AND ANALYSIS

A. Classical transport properties

Figure 1 shows the temperature dependence of the resistivity ρ of two thin $CoSi_2$ layers [115-Å thickness in (111)Si, and 230 Å in (100)Si] measured in the temperature range of 10–200 K. The overall behavior of both samples is consistent with the classical transport for normal metals with $\rho(T) = \rho_0 + \rho_{\mathrm{th}}(T)$ (Matthiessen's rule), where ρ_0 is the residual resistivity usually ascribed to carrier scattering by impurities, structural point defects, etc., and $\rho_{\mathrm{th}}(T)$ is the temperature-dependent contribution due to scattering by phonons. Below ≈ 15 K, the resistivity shows a distinct temperature dependence which is not visible in the scale of Fig. 1. This will be discussed in Sec. IV B.

The temperature dependence of both samples in Fig. 1 shows two interesting features: first, there is a difference in the residual resistance between the samples in the two orientations; and second, the residual resistivity of both samples is shifted to higher values as compared to thick (70–100 nm), bulklike $CoSi_2$ layers. For thick $CoSi_2$ layers, a difference of about 1 $\mu\Omega$ cm was found between the different orientations:[34] $\rho_0 \approx 1$ $\mu\Omega$ cm in (100)Si and $\rho_0 \approx 2$ $\mu\Omega$ cm in (111)Si (all samples formed by mesotaxy). We found $\rho_0 = 2.2\,\mu\Omega$ cm in (100)Si and $\rho_0 = 3.9\,\mu\Omega$ cm in (111)Si for the thin layers, indicating a tendency for the residual resistivity to decrease with increasing thickness. For $CoSi_2$ layers on (111)Si, Hensel *et al.*[4] found a relatively small increase of the residual resistance with decreasing thickness, and attributed this to an essentially classical specular scattering of carriers at the interface. Also, quantum size effects in thin layers were discussed in order to understand the increase in the residual resistance.[6] The residual resistivity in the (111)Si layer is consistently higher than in (100)Si layers, although the minimum yield value (defined as the ratio of the channeled yield to the random yield in a Rutherford backscattering spectrum) of the (111)Si layers is lower, indicating better crystallinity [4% minimum yield in (111)Si, and 8% in (100)Si]. The difference in the residual resistance in our samples is due to two effects: first, a thickness dependence, and, second, a general difference in electrical properties between both orientations, as discussed below.

From ρ_0, we calculated the mean free path l_0 of the two samples using a free-electron model for a first estimation: $l_0 = mv_F/(ne^2\rho_0)$, with m the free-electron mass and n the charge-carrier concentration (see Table I). Due to the 2D character of the films, we used the two-dimensional diffusion constant $D = v_F l_0/2$ (see Table I). Both samples showed superconductivity. The (111)Si had

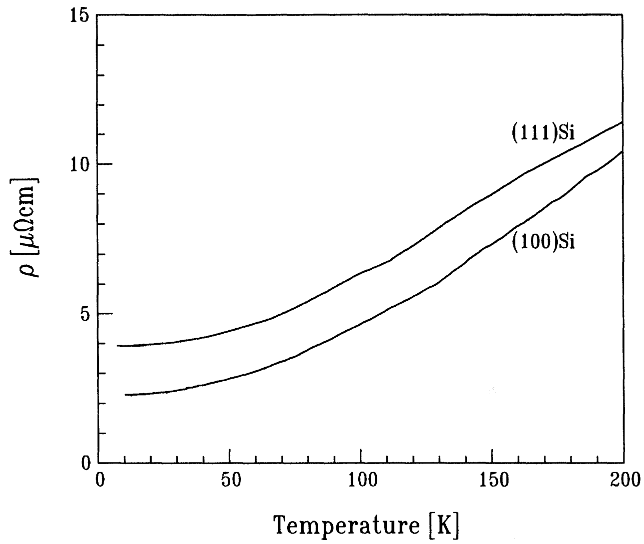

FIG. 1. The plot of resistivity vs temperature for an 11.5-nm-thick $CoSi_2$ layer buried in (111)Si and a 23-nm-thick $CoSi_2$ layer buried in (100)Si. The shape of the curves is similar, indicating that the silicides have the same phonon spectrum in both orientations, but the (100)Si curve falls below the (111)Si curve due to a lower residual resistance.

TABLE I. The residual resistance ρ_0 at 4.2 K of both $CoSi_2$ layers and physical quantities deduced from them (mean free path l_0, elastic scattering time τ_0, and the diffusion coefficient D). T_C is the critical temperature.

Sample orientation	Thickness (nm)	ρ_0 (at 4.2 K) ($\mu\Omega$ cm)	l_0 (nm)	τ_0 ($\times 10^{14}$ s)	$k_F l_0$	D (cm^2/s)	T_c (K)
(111)Si	11.5	3.9	38.4	3.7	348	202	0.85
(100)Si	23.0	2.2	67.6	6.6	612	355	1.455

a relatively broad transition ($\Delta T_C = 0.1$ K and $T_C = 0.85$ K), while the (100) sample had a very sharp transition ($\Delta T_C = 0.003$ K) with $T_C = 1.455$ K (T_C measured at the midpoint).

Another difference in the electrical properties of the two orientations is found in the Hall coefficient R_H (see Fig. 2). In both cases, we measured a positive sign for R_H [$R_H = (ne)^{-1}$] but with a significant difference in the magnitudes. For the (100)Si sample we obtained $R_H = 2.6 \times 10^{-4}$ cm^3 C^{-1} ($\cong n = 2.4 \times 10^{22}$ cm^{-3}), which is temperature independent in the examined temperature range (2–13 K); for the (111)Si sample we found $R_H = 5.9 \times 10^{-4}$ cm^3 C^{-1} which is about two times larger than in (100)Si. A strong orientation dependence of R_H for mesotaxial layers (thickness of about 75 nm) was first measured by Van Ommen *et al.*,[35] but their measured value at low temperature does not agree very well with our measurements [$R_H = 2.1 \times 10^{-4}$ cm^3 C^{-1} in (100)Si and $R_H = 3.7 \times 10^{-4}$ cm^3 C^{-1} in (111)Si]. A similar temperature dependence was also observed by other groups for 50-nm-thick samples.[13] The Hall coefficient shown by these 50-nm-thick samples in (100) orientation was nearly temperature independent, and had a low-temperature value of $R_H = 2.5 \times 10^{-4}$ cm^3 C^{-1}. However, R_H versus T for the (111)-oriented 50-nm-thick samples showed completely different behavior. At room temperature, R_H showed a value similar to that for the (100)-oriented sample, but in an intermediate temperature range (100–250 K) R_H increased to a value of $R_H = 5.0 \times 10^{-4}$ cm^3 C^{-1}. This remained constant below 100 K.

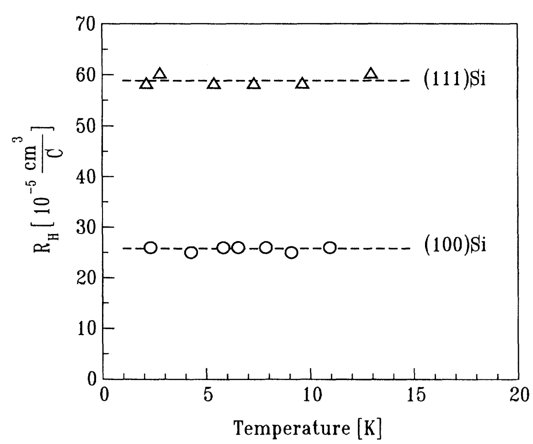

FIG. 2. The Hall coefficient as a function of temperature for the buried $CoSi_2$ layers in (100)Si (23 nm thick) and in (111)Si (11.5 nm).

The dependence of the electrical properties of $CoSi_2$ layers fabricated with mesotaxy on the orientation seems to be general behavior. As pointed out by Vandenberg *et al.*,[34] a comparison of (111), (100), and (110) orientations showed that the lateral mismatches were similar, but the perpendicular mismatch increased monotonically through the series. They further argued that this difference in the degree of relaxation of the three orientations provides a possible explanation for the observed anisotropy in the electrical properties. But the origin of this anisotropy is more probably due to the multiple bands in $CoSi_2$. As mentioned in Sec. III A, three-hole bands contribute in $CoSi_2$ to the electrical transport.[18] In addition, the $CoSi_2$ layers are single crystals and show an epitaxial relationship to the Si substrate. From the literature (see, e.g., Ref. 36), it is known that single crystals show a strong orientation and temperature dependence of the Hall coefficient. This orientation dependence is normally attributed to the topography of the Fermi surface (e.g., open or closed orbits) in a certain orientation. Under this condition, the Hall coefficient depends in detail on the relative band parameters, such as effective mass and mobility in the single bands, and on the number of bands. If the three bands in $CoSi_2$ now contribute with different weights to the charge transport, the orientation dependence of the residual resistance could be understood in the same way as a multiple-band effect.

Since the prefactor of the classical contribution to the magnetoresistance depends on the relative values of the band-structure parameters,[17] we also expect an anisotropy in the magnetoresistance. As shown in Fig. 3, the magnetoresistance is indeed orientation dependent, with a much stronger increase in resistance with increasing magnetic field in (100)Si than in (111)Si. As indicated in the inset, the magnetoresistance shows the H^2 behavior which was also found for thick $CoSi_2$ layers on (111)Si substrates.[4,11] The existence of classical magnetoresistance indicates that more than one conduction band (at least two bands) contributes to the electrical transport, in agreement with the prediction in Sec. III A. For the (111)Si sample (for the details see Sec. IV B) we obtain $\alpha_1 = (1.37 \pm 0.07) \times 10^{-4}$ T^{-2}, and for the (100)Si sample a coefficient one order of magnitude higher, $\alpha_1 = (2.0 \pm 0.03) \times 10^{-3}$ T^{-2}. From these values we can calculate the elastic-scattering time $\tau_0^{(111)\mathrm{Si}} \approx 6.6 \times 10^{-14} (m^*/m)$ s and $\tau_0^{(100)\mathrm{Si}} \approx 2.5 \times 10^{-13} (m^*/m)$ s. These values are 2–4 times as large as those listed in Table I, but the agreement between these values is fairly

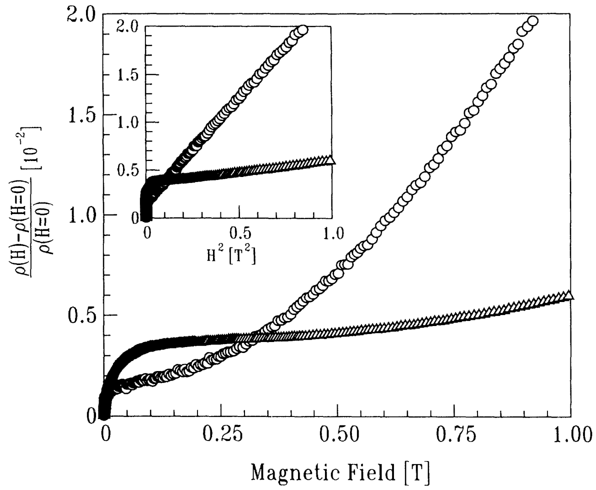

FIG. 3. Magnetoresistance data measured at 4 K for the 11.5-nm-thick buried $CoSi_2$ in (111)Si (triangles) and 23-nm-thick buried $CoSi_2$ in (100)Si (circles). The inset shows a plot of the magnetoresistance vs H^2, indicating the classical H^2 dependence at higher fields. The behavior of the magnetoresistance at lower fields is due to quantum corrections.

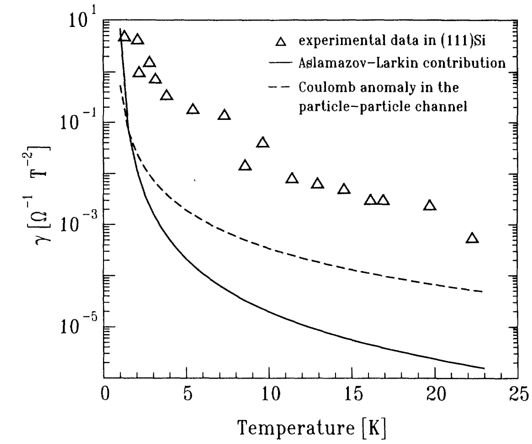

FIG. 4. The logarithm of the value of γ, the coefficient of the quadratic magnetic-field dependence, is plotted vs the temperature. The symbols give the experimental results from the magnetoresistance curves of the $CoSi_2$ layer in (111)Si, shown in Fig. 5(a). These data points are compared to the theoretical contribution of the Aslamazov-Larkin part (using $dH_{C_2}/dT \approx 0.016 \pm 0.002$ T/K and $T_C = 0.85$ K) and that of the Coulomb anomaly in the particle-particle channel. Contributions of the Coulomb anomaly in the particle-hole channel indicated values of γ lower than 10^{-6} $\Omega^{-1} T^{-2}$ and are not considered in this plot.

good considering the crudeness of the model and the quality of the estimated values. As a comparison, a value of $\alpha_1 = 2.1 \times 10^{-4}$ T^{-2} was found by Hensel *et al.*[4] for thick (110 nm) $CoSi_2$ layers on (111)Si substrates, which is close to the measured α_1 for the 11.5-nm-thick $CoSi_2$ in (111) Si.

The observation of a classical contribution to the magnetoresistance is not surprising because our samples are relatively clean: $k_F l_0 \gg 1$, with a sheet resistance $R_{Sh} \approx 1$ Ω. At lower magnetic fields, the magnetoresistance data in Fig. 3 is influenced by quantum interference effects, as will be discussed in Sec. IV B. These classical contributions are generally not discussed in studies of localization in much dirtier systems ($k_F l_0 \approx 1$), because these quantum contributions dominate.

B. Quantum effects in two-dimensional $CoSi_2$ films

1. Calculation and comparison of Aslamazov-Larkin contribution and interaction effects with the experimental data

Before we discuss the analysis of the magnetoresistance data, it is useful to estimate the magnitude of the different corrections as a function of temperature. As discussed in Sec. III, the magnetoresistance shows a quadratic-field dependence ($\Delta R / R_0^2 \approx \gamma \xi H^2$) to lowest order in H [see Eqs. (6), (9), (10), and (11) for the coefficients of $\gamma(T)$], which is determined experimentally and compared to the different possible corrections.

To estimate the AL contribution, we measured $dH_{C_2}/dT \approx 0.016$ T/K, with $T_C = 0.85$ K for the (111)Si sample. Using these values, we calculated the prefactor $\gamma_{AL}(T)$ in Eq. (9), and plotted it versus temperature in Fig. 4. In addition, we also fitted a parabola to the experimental data at very low magnetic fields and plotted the experimental values for $\gamma(T)$ in Fig. 4. The experimental data were obtained in a magnetic-field region from 0 to 50 G, depending on the temperature. In contrast, the classical H^2 dependence becomes dominant at much higher magnetic fields ($> \approx 0.4$ T, depending on the orientation) and has no influence in the determination of $\gamma(T)$. A comparison of the experimental values and calculated values indicate that we can safely ignore the Aslamazov-Larkin term in our analysis if we perform our experiments in a temperature regime of $T/T_C > 1.4$. A similar temperature region, where the Aslamazov-Larkin contribution can be neglected, is also found for Al films.[37]

A similar procedure was performed for the Coulomb interaction terms. For the interaction in the particle-hole channel using Eq. (10) we obtained a prefactor of the H^2 term yielding values of 4.7×10^{-7} $\Omega^{-1} T^{-2}$ for 1 K and 2.9×10^{-8} $\Omega^{-1} T^{-2}$ for 4 K which is at least six orders of magnitude smaller than the experimental data in Fig. 4, indicating that interaction effects in the particle-hole channel can be neglected in our analysis.

The calculated prefactor in the particle-particle channel is also plotted in Fig. 4 [Eq. (11)]. A comparison with the experimental data indicate that the measured values are at least one order of magnitude higher than the prediction of Eq. (11), an indication that Coulomb interactions in the particle-particle channel are also not a significant contribution to the magnetoresistance in $CoSi_2$ films.

The fact that the Coulomb interaction is not a significant quantum correction in $CoSi_2$ films is consistent with the measured temperature independence of the Hall coefficient R_H (see Fig. 2). If only localization effects are important, R_H should be independent of temperature,[19,38] even in the case of strong spin-orbit scattering.[39] If interaction effects were dominant, the fractional change in R_H would be twice the fractional change in resistance over the whole temperature range:[19,38]

$$\frac{R_H(T)-R_H(T_0)}{R_H(T_0)}=2\frac{R(T)-R(T_0)}{R(T_0)}, \tag{12}$$

where all quantities are measured at the same magnetic field. Equation (12) is only valid in the case of dominant Coulomb interaction effects, but, in the presence of both interaction and localization effects, the theory predicts a temperature dependence of R_H. The data in Fig. 2 show that there is no change in R_H in almost a decade in temperature. For quantum corrections to the electronic transport in $CoSi_2$ layers, this suggests that single-particle localization is mainly responsible in this temperature and magnetic-field range.

2. Two-dimensional weak localization and Maki-Thompson contribution

Figures 5(a) and 5(b) show the magnetoresistance normalized to ξ at different temperatures for the (111)Si and (100)Si samples. The magnetoresistance data show regions where ΔR is proportional to $\ln(H)$ in an intermediate range of H. A $\ln(H)$ dependence is characteristic of localization and interaction effects in two-dimensional disordered systems:

$$\frac{\Delta R}{R_0^2}=\xi\alpha_H\ln(H)+\text{const} . \tag{13}$$

The term α_H can be written to first approximation as $\alpha_H=\alpha_{ee}+\alpha_{wl}$, where α_{ee} is the contribution from interaction effects and α_{wl} is from weak localization effects.[40] Estimate for α_{ee} indicate maximum values of 0.08 at 1 K and 0.1 at 10 K, calculated with $F=1$ and values of 0.033 at 1 K and 0.036 at 10 K, calculated with $F=0.1$.[41] The theory of weak localization predicts a value of $\alpha_{wl}=0.5$ (Ref. 42) in the case of strong spin-orbit scattering. Figure 6 shows the experimentally obtained values of α_H for the different temperatures and orientations. The prefactors α_H were determined in the regions where ΔR is approximately proportional to $\ln(H)$. For a temperature range of 1 to ≈ 10 K, we obtained a $\alpha_H=(0.5\pm0.05)$ for both samples, indicating the dominance of weak localization with strong spin-orbit scattering in this temperature region. There is a smooth decrease of α_H above 10 K, but it remains larger than α_{ee} over the whole investigated temperature range. This is an additional evidence for our conclusion in Sec. IV B 1 that Coulomb interaction effects are not important in $CoSi_2$ layers. The decrease of α_H with temperature above ≈ 10 K indicates that spin-orbit scattering effects become less important at higher temperatures. At higher temperatures, the weak localization becomes more important, leading to a decrease in α_H [the theory of weak localization with weak spin-orbit scattering predicts $\alpha_H=-1$ (Ref. 42)].

As pointed out in Sec. III C the validity of Eq. (4) for the MT contribution is restricted to low magnetic fields [Eqs. (5a) and (5b)]. The calculation of the validity of Eq. (4) for our $CoSi_2$ film in (111)Si, using relation (5b), indicates that Eq. (4) is only applicable for $H \ll 18$ G at 2 K, and for $H \ll 260$ G at 10 K. An estimate of the MT contribution to the resistance was done by using Eq. (6) for the values of $\gamma(T)$ at low magnetic fields. The theoretical curvature is $\gamma=1.15\times10^{-6}\ \Omega^{-1}\mathrm{T}^{-2}$ for 2 K and $\gamma=1.39\times10^{-7}\ \Omega^{-1}\mathrm{T}^{-2}$ for 10 K. These values indicate a curvature too small by several orders of magnitude

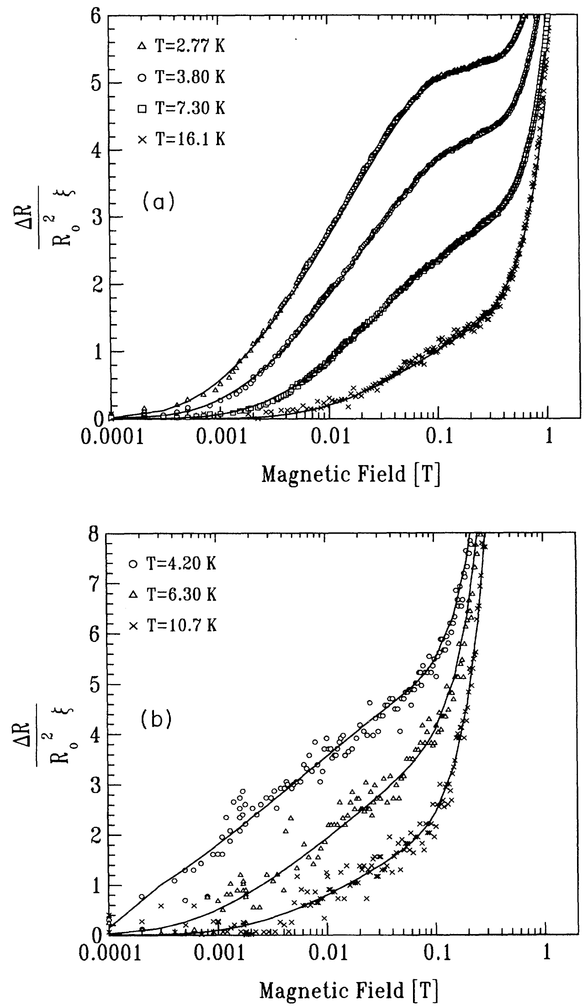

FIG. 5. (a) The normalized magnetoresistance of buried $CoSi_2$ in (111)Si (thickness 11.5 nm) at different temperatures. The fits (solid lines) were performed using weak localization theory, with a contribution of the classical, temperature-independent H^2 term. Contributions due to superconducting fluctuations (Aslamasov-Larkin and Maki-Thompson) are negligible in the investigated temperature region. (b) The normalized magnetoresistance of buried $CoSi_2$ in (100)Si (thickness 23 nm) at different temperatures. Weak localization theory and a classical contribution were only used to perform the fits (solid lines).

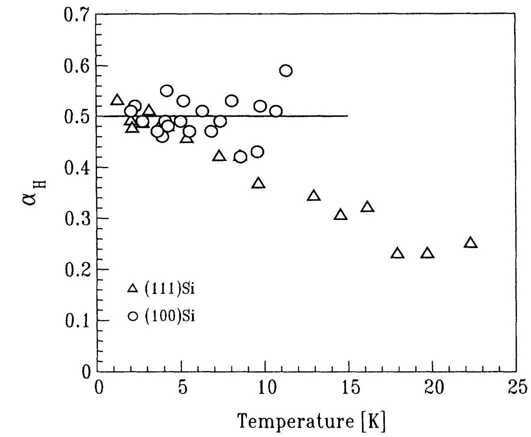

FIG. 6. Experimental prefractors α_H of the ln(H) dependence of the magnetoresistance [Eq. (13)] at different temperatures.

compared to the data in Fig. 4, which is an indication that MT contributions do not dominate at low magnetic fields in a temperature region above twice the critical temperature T_C. Fortunately the further analysis of the data is consistent with the assumption that MT contributions are not important for temperatures above ≈ 2 K for the (111)Si sample due to suppression of superconducting fluctuation in very low fields (< 150 G) (see also Sec. IV B 3).

The magnetoresistance data were symmetrical for positive and negative applied magnetic fields. There were slight variations (≈ 10 G) in the position of the minimum in field, due to some hysteresis in the magnet. The true zero of magnetic field was estimated by finding the resistivity minimum in a low-field sweep. The fitting of the data in Figs. 5(a) and 5(b) to the theoretical expression [sum of Eqs. (1) and (2a)] was performed in three steps.

First we fitted the data from 0 to 1 T, with $H_{\rm s.o.}$, $H_{\rm in}$, H_s, and the classical prefactor α_1 as the free parameter. If magnetic scattering were dominant in our samples, we would expect a temperature independent scattering rate due to the fact that τ_s, which determines the phase breaking time, is not temperature dependent.[43] This was observed by DiTusa, Parpia, and Phillips[9] for very thin $CoSi_2$ layers (< 12 nm). For thicker layers (20 nm), they observed a stronger temperature dependence, indicating that τ_s is no longer the phase breaking scattering time. However, since we see a strong temperature-dependent contribution [Figs. 5(a) and 5(b)] to the magnetoresistance data, we expect that, in mesotaxial $CoSi_2$ layers, magnetic scattering is small. This is also confirmed by the fitting procedures. The best quality of the fits was obtained by negative H_s, but this has no physical meaning. Due to both results, the strong temperature dependence of the magnetoresistance data and inconsistency in the fits, we conclude that $H_s \ll H_{\rm in}$ and $H_s \ll H_{\rm s.o.}$. In the following analysis we set $H_s = 0$. From the fits from 0 to 1 T, we obtain the prefactor for the classical contribution, as already discussed in Sec. IV A.

After this first fit, a second fit from 0 to 0.4 T was performed, with $H_{\rm s.o.}$ and $H_{\rm in}$ as free parameters. From this series of fits we obtained the spin-orbit scattering time $\tau_{\rm s.o.}$ for the different temperatures, plotted in Fig. 7. As seen in Fig. 7, $\tau_{\rm s.o.}$ is essentially temperature independent within the experimental error, where the error increases with rising temperature due to the decreasing importance of localization effects. For the (111)Si sample, the average spin-orbit scattering rate is $\langle \tau_{\rm s.o.} \rangle = (1.5 \pm 0.3) \times 10^{-13}$ s, and for the (100) Si sample, a slightly higher value of $\langle \tau_{\rm s.o.} \rangle = (1.6 \pm 0.4) \times 10^{-13}$ s is found. These values are in reasonable agreement with $\tau_{\rm s.o.} \approx 2 \times 10^{-13}$ s found by DiTusa, Parpia, and Phillips[9] for $CoSi_2$ layers formed on (111)Si substrates. For single-crystalline $NiSi_2$ Matsui *et al.*[8] found a spin-orbit scattering time, about one order of magnitude larger ($\tau_{\rm s.o.} \approx 1 \times 10^{-12}$ s). An estimate of the importance of the spin-orbit scattering rate in metals, without considering boundary effects, is given by Abrikosov and Gorkov:[44]

$$\frac{\tau_0}{\tau_{\rm s.o.}} = (\alpha Z)^4 , \tag{14}$$

where α is the fine-structure constant ($\approx \frac{1}{137}$), Z is the atomic number ($Z = 27$ for Co and 14 for Si), and τ_0 the elastic-scattering rate obtained from resistance measurements. Assuming that the spin-orbit scattering is dominated by the Co atoms, Eq. (14) predicts $\tau_0/\tau_{\rm s.o.} \approx 1.5 \times 10^{-3}$. Experimentally, we obtained $\tau_0/\tau_{\rm s.o.} \approx 0.25$ in (111)Si and $\tau_0/\tau_{\rm s.o.} \approx 0.39$ in (100)Si, indicating a much stronger spin-orbit scattering in $CoSi_2$ films than expected from Eq. (14). The origin of this strong spin-orbit scattering is unclear, since to our knowledge there exists no theoretical description of such a strong spin-orbit scattering.

After determining $\tau_{\rm s.o.}$, $H_{\rm s.o.}$ was also fixed, and the magnetoresistance data were fitted a third time from 0 to 0.4 T using one fitting parameter $H_{\rm in}$. The fitted inelastic-scattering times $\tau_{\rm in}$ and the inelastic-scattering lengths $l_{\rm in} = (D\tau_{\rm in})^{1/2}$ (=phase coherent length l_ϕ) are plotted in Figs. 8(a) and 8(b), respectively. Different powers for the temperature dependence of $\tau_{\rm in}$ were found

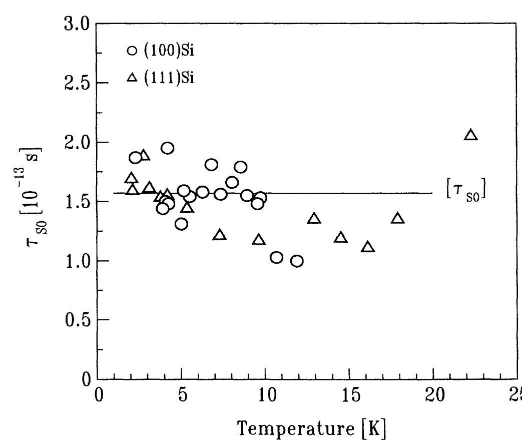

FIG. 7. The spin-orbit scattering time of buried $CoSi_2$ layers in (111)Si and (100)Si as a functon of temperature.

for the two $CoSi_2$ layers: in (111)Si, $\tau_{in} \propto T^{-1.1}$ up to ≈ 6 K, and a stronger decrease at higher temperatures; in (100)Si a similar dependence is observed, $\tau_{in} \propto T^{-1.1}$ to ≈ 5 K and above, also a stronger decease with temperature. The scatter of the data, especially at higher temperatures, is due to noisy data [see Fig. 6(b)], which complicates the analysis at these temperatures, especially in the (100)Si sample. The crossover of the different power laws (transition temperature T_t) is slightly shifted to lower temperatures for the (100)Si sample, compared to (111)Si which is consistent with its lower resistivity (see Table I). Similar behavior was found for single-crystalline $NiSi_2$ layers, where T_t is shifted to lower temperatures with decreasing resistivity of the layers.[8] Also, the τ_{in} obtained for $CoSi_2$ in (100)Si are comparable to the values found by Matsui *et al.*[8] for $NiSi_2$ but since the coherence length $l_\phi = (D\tau_\phi)^{1/2} = (D\tau_{in})^{1/2}$, the l_ϕ obtained are larger for $CoSi_2$ layers than for $NiSi_2$, due to the larger diffusion coefficient D corresponding to the lower resistivity. In addition, a comparison of the inelastic-scattering time in (111)Si in the temperature range from 1 to 2 K, with the values of thick $CoSi_2$ layers (20 nm), measured by DiTusa, Parpia, and Phillips[9] ($\tau_{in} \approx 10^{-10}$ s) shows a reasonable agreement.

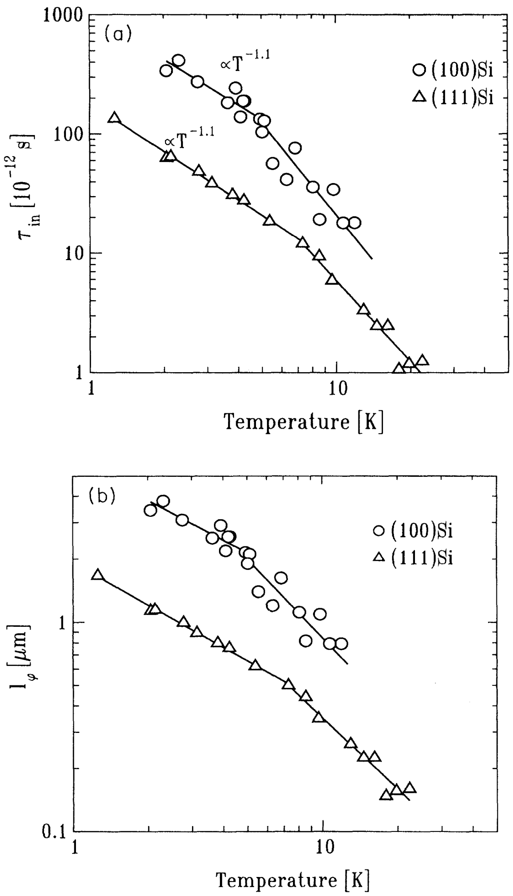

FIG. 8. (a) Inelastic-scattering time τ_{in} (phase breaking time τ_ϕ) vs temperature for two buried $CoSi_2$ samples. (b) Phase-coherence length l_ϕ [inelastic scattering length $l_{in} = (D\tau_{in})^{1/2}$] as a function of temperature for $CoSi_2$ layers in (111)Si and (100)Si.

There are two possible mechanisms causing a dephasing of charge carriers in two dimensions: electron-phonon scattering with the scattering rate $\tau_{e\text{-ph}}^{-1}$, and electron-electron scattering with the rate $\tau_{e\text{-}e}^{-1}$. These will be discussed below.

According to the theory of electron-electron interaction in a 2D weakly localized regime, τ_{in} is given by[45–48]

$$\tau_{in}^{-1} = \frac{k_B T}{2E_F\tau_0} \ln\left[\frac{2\pi E_F \tau_0}{h}\right] \quad \text{for } k_B T < h/(2\pi\tau_0)\ , \qquad (15a)$$

$$\tau_{in}^{-1} = \frac{\pi^3 k_B^2 T^2}{hE_F} \ln\left[\frac{E_F}{k_B T}\right] \quad \text{for } k_B T > h/(2\pi\tau_0)\ . \qquad (15b)$$

Equation (15a) gives a linear temperature dependence (τ_{in} proportional to T^{-1}), and (15b) shows that τ_{in}^{-1} is effectively proportional to T^2, since the logarithm varies much more slowly in T than T^2. The calculation of the transition temperature T_t [$=h/(2\pi k_B \tau_0)$] between the Eqs. (15a) and (15b) regions for the (111)Si and (100)Si samples indicates $T_t \approx 209$ and 120 K, respectively, indicating that only Eq. (15a) is only valid for our conditions. Calculation of the inelastic-scattering times using Eq. (15a) [with $E_F = 6.2$ eV for $CoSi_2$ (Ref. 18)] shows that, at 4 K, $\tau_{in} = 1.9 \times 10^{-11}$ and 3.5×10^{-11} s for the (111)Si and (100)Si samples, respectively. This is in reasonable agreement with the experimental data of $\tau_{in}^{exp} = 3.0 \times 10^{-11}$ s and $\tau_{in}^{exp} = 1.5 \times 10^{-10}$ s, respectively [see Fig. 5(a)]. This tendency shows that the inelastic-scattering rate increases with the disorder, i.e., proportional to τ_0^{-1} or proportional to the resistivity, but, since the measured inelastic scattering times are smaller than predicted by Eq. (15a), there must be an additional scattering mechanism. Also, the origin of the crossover temperature is not due to the transition between the validity of Eqs. (15a) to (15b) of the electron-electron scattering, as found for $NiSi_2$.[8]

For Al films, it was found that τ_{in}^{-1} is dominated by electron-phonon scattering at higher temperatures.[26,37] In order to estimate the influence of electron-phonon scattering, we need to obtain the dimensionality of the system with respect to the electron-phonon scattering. For this the physical dimensions of the system are compared with the most probable phonon wavelength, $\lambda_{ph} = 2\pi/q_{ph}$, where $q_{ph} = 2k_B T/(ch)$ is the characteristic phonon wavelength, and c the velocity of sound.[37] To our knowledge, c has not been measured for $CoSi_2$, but to estimate q_{ph} we calculated c with the Bohm-Staver relation[49] to $c \approx 2500$ m/s. We obtained $\lambda_{ph} \approx 37$ nm/T (T in K). Therefore, our $CoSi_2$ samples are in the clean limit ($q_{ph} l_0 > 1$) of electron-phonon scattering, indicating three-dimensional (bulk) behavior. Most calculations of the electron-phonon-scattering rate were performed in the dirty limit ($q_{ph} l_0 < 1$) and normally predicted a rate proportional to T^2, e.g., see Ref. 50. But the calculation of the scattering rates for our samples using this theory yielded values about six orders of magnitude higher than those plotted in Fig. 8(a), an indication that the theories in the dirty limit are not applicable for $CoSi_2$. In order to estimate the temperature dependence, we fitted the experimental scattering rates to a function of the form $\tau_{\text{in}}^{-1} = A_1 T + A_3 T^n$. The fits were performed for $n=2$, 3, and 4, where the best fit was obtained for $n=3$:

$$\tau_{e\text{-ph}}^{-1} = A_3 T^3 \approx 8\times 10^7 T^3 \ , \qquad (16)$$

where A_3 is not strongly orientation dependent. A similar temperature dependence was obtained for Al film, which was also in the clean limit of the electron-phonon scattering.[26,37] Up to now there has been no theoretical calculation of the electron-phonon scattering rate where the microscopic band-structure parameters were used for comparison with the result in Eq. (16). The values of A_1 obtained from the fit of $A_1^{(111)\text{Si}} = 7.9\times 10^9\ \text{K}^{-1}\text{s}^{-1}$ and $A_1^{(100)\text{Si}} = 1.2\times 10^9\ \text{K}^{-1}\text{s}^{-1}$ are also in agreement with the prediction of Eq. (15a): $A_1^{(111)\text{Si}} = 1.1\times 10^9\ \text{K}^{-1}\ \text{s}^{-1}$ and $A_1^{(100)\text{Si}} = 6.8\times 10^8\ \text{K}^{-1}\text{s}^{-1}$. This discussion proves that the inelastic scattering is due to a combination of electron-electron-scattering and electron-phonon-scattering processes, such that $\tau_{\text{in}}^{-1} = \tau_{e\text{-}e}^{-1} + \tau_{e\text{-ph}}^{-1}$.

To check the validity of our estimate in Sec. IV A, we plotted the same parabolic fits to the magnetoresistance at low magnetic fields for the (111)Si and (100)Si samples in Fig. 9, and compared them to the theoretical contribution of weak localization with strong spin-orbit scattering using Eq. (3) alone. For the temperature dependence, $H_{\text{in}} = H_{\text{in}}(T) = h/(8\pi e D \tau_{\text{in}}(T))$ was used, where the temperature dependence of the inelastic-scattering time is given in Fig. 8(a). Considering the roughness of the validity of Eq. (3) and the experimental error, the temperature dependence of γ is well described by the localization theory alone, indicating the dominance of this quantum effect in the temperature range investigated.

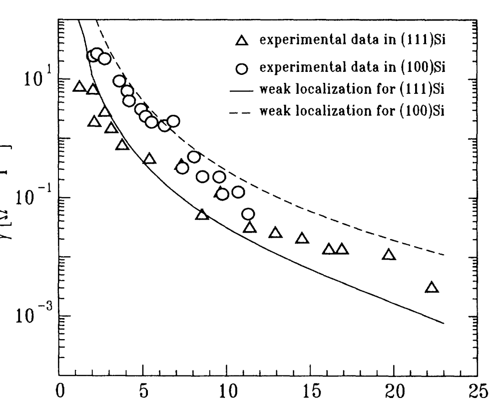

FIG. 9. The logarithm of the value of γ, the coefficient of the quadratic magnetic-field dependence for $CoSi_2$ in (111)Si and (100)Si, is plotted vs the temperature. These data points are compared to the theoretical contribution of the weak localization, which shows a reasonable agreement with the roughness of the estimations.

3. *Temperature dependence of the resistivity*

In early experiments on localization, thin films of nonsuperconducting metals were used and a resistance increase with decreasing temperature was observed. This increase is also observed in $CoSi_2$ layers which showed no superconductivity.[9,51] According to both localization and interaction theories, the change in the 2D resistivity of two-dimensional systems in the weakly localized regime from temperature T to T_0 is given by[24]

$$\frac{\Delta R(H,T)}{R_0^2} = \frac{R(H,T) - R(H=0,T_0)}{R(H=0,T_0)^2} = -\xi \alpha_T \ln\left[\frac{T}{T_0}\right] + \text{const} \ . \qquad (17)$$

In Fig. 10, $\Delta R/R_0^2$ is plotted versus $\log(T/T_0)$ normalized at $H=0$ to $T_0 = 3.8$ K. In zero magnetic field, we observe no increase with decreasing temperature. However, since our samples show superconductivity, the resistance decreases with T at the lowest temperatures probably due to MT superconducting fluctuations. A magnetic field of $H \approx 150$ G is enough to suppress the influence of superconducting fluctuations, and we clearly see a logarithmic increase of resistance with decreasing temperature. The experimentally determined α_T [obtained in the regions where ΔR is approximately proportional to $\ln(T)$] are plotted in Fig. 11 as a function of applied magnetic field for the (111)Si sample. At zero magnetic field, α_T is negative, but becomes positive at ≈ 100 G. For $H > 200$

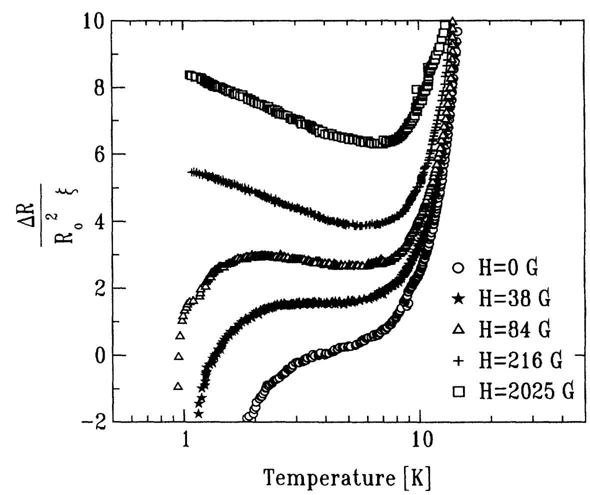

FIG. 10. The low-temperature dependence of the normalized resistance on T for the 11.5-nm-thick buried $CoSi_2$ layer in (111)Si at different applied magnetic fields. All resistance data were normalized to the resistance in zero field at $T=3.8$ K. In zero magnetic field the resistance decreases with temperature due to superconducting fluctuation. These superconducting contributions are suppressed with increasing magnetic field. A magnetic field of ≈ 150 G is enough to suppress all superconducting influence, and a logarithmic increase of the resistance with decreasing temperature is observed, characteristic of weak localization.

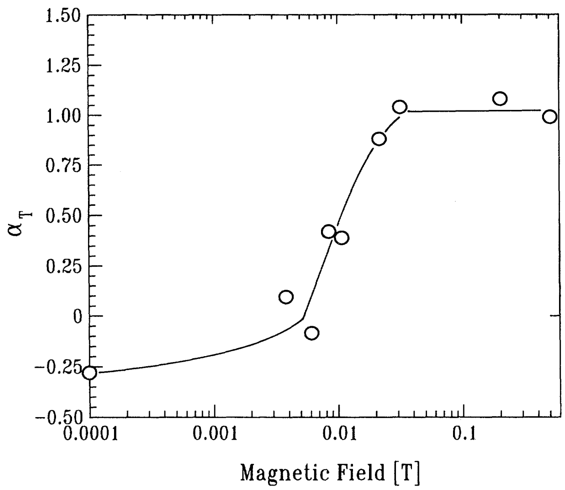

FIG. 11. Experimental prefactor α_T of the $\ln(T)$ dependence of the magnetoresistance [Eq. (17)] at different applied magnetic fields.

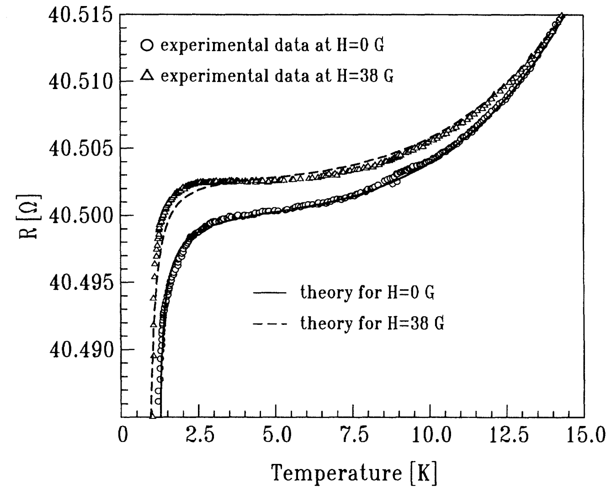

FIG. 12. Resistance vs temperature for the two-dimensional $CoSi_2$ layer in (111)Si. The theoretical fit was matched to the experimental data at $T=3.8$ K. The prefactor for the electron-phonon scattering was used as the only fitting parameter (for details see text).

G, we observed a value of $\alpha_T=0.99\pm0.07$ for magnetic fields up to 0.5 T. This slope is consistent with measurements of DiTusa, Parpia, and Phillips,[9] who measured a slope of $\alpha_T=1.0\pm0.05$ at all fields up to 4 T. The temperature dependence of the factor α_T is predicted by the two theories (localization with strong spin-orbit scattering and interaction);[7,40] in zero magnetic field,

$$\frac{\Delta R}{R_0^2}\left[\frac{\Delta R}{R_0^2}\right]_{\rm loc}+\left[\frac{\Delta R}{R_0^2}\right]_{\rm interact} =\left\{-\left[\frac{p}{2}\right]+[1-\tfrac{3}{4}F]\right\}\xi\ln\left[\frac{T}{T_0}\right], \tag{18}$$

and in magnetic fields much higher than $h/(8\pi De\tau_{\rm in})$ and $4\pi k_B T/(g\mu_B)$,

$$\frac{\Delta R}{R_0^2}=\left[\frac{\Delta R}{R_0^2}\right]_{\rm loc}+\left[\frac{\Delta R}{R_0^2}\right]_{\rm interact} =\{0+[1-\tfrac{1}{4}F]\}\xi\ln\left[\frac{T}{T_0}\right]. \tag{19}$$

In Eqs. (18) and (19), $\tau_{\rm in}$ is assumed to be proportional to T^{-p} (see Sec. IV B 2). The negative prefactor $-p/2$ in Eq. (18) signifies that the effect is antilocalization. A comparison of the experimental α_T at higher magnetic field to Eq. (19) indicates that the screening parameter F is very small ($F\leq0.04$), and from Eq. (18) we obtain $p\approx2.5$. $F\approx0$ is additional evidence of the conclusion that Coulomb interaction effects are not dominant in $CoSi_2$.

The experimental data for the temperature dependence of $\Delta R/R_0$ for the (111)Si sample in the temperature range from 0 to 15 K are shown in Fig. 12. The theoretical fits include the contribution from classical electron-phonon scattering, localization, and Maki-Thompson fluctuations. Contributions from electron-electron scattering are assumed to be negligible. The data are shown for zero field and for a magnetic field of 38 G. The best fit at zero field was obtained by using Eq. (8) for the Maki-Thompson contribution. The fit at 38 G was done by using Eq. (4) as a first approximation for the MT contribution; however, since this theory is no longer valid for such "high" magnetic fields, we get a poorer fit as compared to the zero-field case. MT corrections were used at higher temperatures since the Aslamazov-Larkin contributions normally dominate only in the vicinity of T_c. Fitting at higher fields was not possible due to the lack of theoretical description in this field region (see Sec. IV B 2). The phonon contribution is well fitted by $\Delta R/R_0=C_{\rm ph}T^3$ ($C_{\rm ph}\approx2\times10^{-6}$ K^{-3}) in the temperature range from 1 to 15 K. This T^3 dependence is also observed for $CoSi_2$ layers in the temperature-dependent part of Matthiessen's rule in a range from 4 to 300 K.[15,52] In these investigations, the T^3 dependence was interpreted as s-d electron-phonon scattering between overlapping energy bands, which seems likely since band-structure calculations of $CoSi_2$ have indicated overlapping s-d bands.[18,53] A scattering rate proportional to T^3 is also obtained for temperatures well below the Debye temperature [Debye temperature for $CoSi_2$: $\Theta_D\approx530$ K (Refs. 15 and 52)] if a large amount of umklapp scattering is assumed, where the charge-carrier velocity and the momentum can change by a large amount for a small change in k.[17] In this case, the determined $C_{\rm ph}$ should be related to the value of A_3, the prefactor for the electron-phonon scattering rate (Sec. IV B 2:[37] $C_{\rm ph}=A_3 l_0/v_F$. This formula is valid if all scattering events contribute to the resistance and there is no restriction to small scattering angles. The absence of this restriction on scattering angles is an indication that umklapp scattering is significant in $CoSi_2$, as also found for thin Al films.[37] With the above formula, we find $A_3\approx5.5\times10^7$ T^{-3} s^{-1}, which is in reasonable agreement with the measured value of

$A_3 \approx 8\times10^7\ \mathrm{T}^{-3}\,\mathrm{s}^{-1}$ in Sec. IV B 2.

For the fits, the values and temperature dependencies of H_{in} and $H_{s.o.}$ were determined in Sec. IV B 2 by magnetoresistance measurements, and C_{ph} was taken as the only fitting parameter. Figure 13(a) shows the resistance change in a zero field decomposed into the individual contributions. The general shape of the $R(T)$ curve at higher temperatures (above 6 K) is due to the dominance

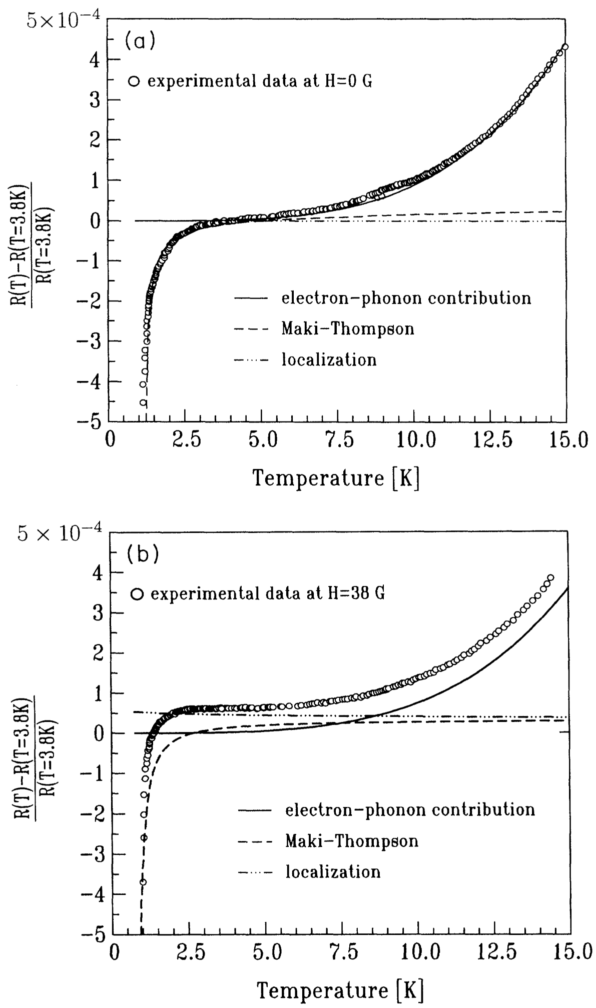

FIG. 13. (a) The decomposition of the temperature dependence of the resistance at zero field for the $CoSi_2$ layer in (111)Si into individual components (the reference temperature is 3.8 K). The localization contribution (dashed-dotted line) is very small. For $T>6$ K the electron-phonon term is dominant, and for $T<3$ K the Maki-Thompson term of superconducting fluctuation is dominant. In a medium-temperature range (3 K $<T<6$ K), all the terms are comparatively small. (b) Decomposition of $R(T)$ for the $CoSi_2$ layer in an applied magnetic field of 38 G. Relative to the zero-field case, the contribution of the localization at low temperatures [Fig. 13(a)] is clearly enhanced. Superconducting fluctuations are only dominant for temperatures lower than 1.5 K; the electron-phonon contribution is dominant above 9 K. For 1.5 K $<T<$ 9 K, the localization terms are dominant.

of the electron-phonon-scattering contribution (proportional to T^3). Superconducting fluctuations (Maki-Thompson contribution) become important at temperatures below 3 K. In the intermediate temperature region (3 K $<T<6$ K), all terms are small and of comparable magnitude. An estimate of the contribution of weak localization to the fractional change in resistance indicates an increase in the resistance of only $\approx 1\times10^{-5}$ in the whole temperature range. This changes dramatically when a magnetic field of only 38 G is applied, as shown in Fig. 13(b). Relative to the zero-field case, the contribution of the weak localization is clearly enhanced and dominates $R(T)$ in the temperature range from 1.5 to 9 K. The Maki-Thompson contributions dominate for temperatures below ≈ 1.5 K, and the electron-phonon contribution dominates for temperatures above 9 K. A simulation for higher magnetic fields was not possible due to the lack of an appropriate theory for the superconducting contributions. But these fits clearly show that, with increasing magnetic field, the superconducting fluctuations are suppressed and that, above a magnetic field of ≈ 150 G, the superconductivity is completely suppressed. This suppression of superconducting fluctuations at relatively low magnetic fields confirms our assumption that Maki-Thompson contributions are not important in the analysis of magnetoresistance data at temperatures above ≈ 2 K [see Fig. 6(a)].

From this discussion, we conclude that electron-phonon scattering is responsible for the inelastic scattering at higher temperatures, and explains both the magnetoresistance and the $R(T)$ dependence.

V. CONCLUSIONS

A strong anisotropy in the electrical properties was determined for mesotaxial $CoSi_2$ in (111)Si and (100)Si. The residual resistance of $CoSi_2$ in (111)Si is always about 1 $\mu\Omega$ cm higher than in (100)Si. The Hall coefficient R_H of (111)Si was found to be $R_H=5.9\times10^{-4}$ cm^3 C^{-1} and $R_H=2.6\times10^{-4}$ cm^3 C^{-1} in (100)Si over a temperature range from 2 to 13 K (values are temperature independent in this temperature range). In addition, the prefactor of the classical contribution to the normalized magnetoresistance, which is proportional to H^2, was found to be $\alpha_1=(1.37\pm0.07)\times10^{-4}\ \mathrm{T}^{-2}$ in (111)Si and about one order of magnitude higher in (100)Si, with $\alpha_1=(2.0\pm0.03)\times10^{-3}\ \mathrm{T}^{-2}$. This anisotropy is probably due to a multiple-band effect in single-crystalline $CoSi_2$, and due to different topologies of the Fermi surface in different orientations.

A logarithmic magnetic-field dependence of the resistance was observed in single-crystalline, mesotaxial $CoSi_2$ layers in (111)Si and (100)Si. The coefficient of the $\ln(H)$ term of the resistance change was determined to be $\alpha_H=(0.5\pm0.05)$ in a temperature range from 2 to 11 K; above 11 K, the coefficient in (111)Si decreases with temperature. The temperature dependence of the resistance showed a transition depending on the applied magnetic field: at zero field, the resistance decreases with temperature due to superconducting fluctuations; by applying a magnetic field of about ≈ 150 G, the superconducting fluctuations are completely suppressed and a logarithmic temperature dependence was observed. Above ≈ 150 G, the coefficient of the $\ln(T)$ term was found to be $\alpha_T = 0.99 \pm 0.05$, independent of the applied magnetic field. All these results are consistent with the assumption that the dominant quantum corrections in $CoSi_2$ are due primarily to weak localization with strong spin-orbit scattering. For the spin-orbit scattering time, we obtained values of $\langle \tau_{s.o.} \rangle = (1.5 \pm 0.3) \times 10^{-13}$ s in (111)Si and $\langle \tau_{s.o.} \rangle = (1.6 \pm 0.4) \times 10^{-13}$ s in (100)Si. Coulomb interaction effects and magnetic scattering were found not to be important for quantum transport in $CoSi_2$. Also, the superconducting fluctuation can be neglected at temperatures above ≈ 2 K.

The inelastic-scattering time τ_{in} as a function of temperature was obtained for each sample from the magnetoresistance data by fitting with weak localization theory and classical contribution. The τ_{in} obtained is approximately proportional to $T^{-1.1}$ for both orientations in a lower temperature region ($< \approx 6$ K) and showed a stronger temperature dependence at higher temperatures. To identify the mechanism of the inelastic scattering, τ_{in} is fitted to a power law in temperature. Best fitting was obtained for $\tau_{\text{in}}^{-1} = A_1 T + A_3 T^3$. This behavior could be interpreted as showing that the inelastic scattering is due to a combination of electron-electron (scattering time $\tau_{e\text{-}e}$) and electron-phonon (scattering time $\tau_{e\text{-ph}}$) processes, such that $\tau_{\text{in}}^{-1} = \tau_{e\text{-}e}^{-1} + \tau_{e\text{-ph}}^{-1}$.

The measured, relatively long coherent length l_ϕ of about 2.3 μm at 4 K in (100)Si indicates the potential of single-crystalline $CoSi_2$ for exploring quantum interference effects, and the fabrication of microstructure devices in which quantum effects play an essential role.

ACKNOWLEDGMENTS

We would like to thank J. F. DiTusa for helpful discussions of the magnetoresistance data.

---

[1] S. P. Murarka, *Silicides for VLSI Applications* (Academic, New York, 1983).

[2] P. A. Lee and T. V. Ramakrishnan, Rev. Mod. Phys. **57**, 287 (1985).

[3] S. Washburn and R. A. Webb, Adv. Phys. **35**, 375 (1986).

[4] J. C. Hensel, R. T. Tung, J. M. Poate, and F. C. Unterwald, Phys. Rev. Lett. **54**, 1840 (1985).

[5] J. M. Phillips, J. L. Batstone, J. C. Hensel, and M. Cerullo, App. Phys. Lett. **51**, 1895 (1987).

[6] Z. Tesanivic, M. V. Jaric, and S. Maekawa, Phys. Rev. Lett. **57**, 2760 (1986).

[7] See, e.g., S. Kobayashi and F. Komori, Prog. Theory. Phys. Suppl. **84**, 224 (1985), and references therein.

[8] M. Matsui, T. Ohshima, F. Komori, and S. Kobayashi, J. Appl. Phys. **67**, 6368 (1990).

[9] J. F. DiTusa, J. M. Parpia, and J. M. Phillips, Appl. Phys. Lett. **57**, 452 (1990); Physica B **165&166**, 863 (1990).

[10] P. A. Badoz, A. Briggs, E. Rosencher, F. Arnaud d'Avitaya, and C. d'Anterroches, Appl. Phys. Lett. **51**, 3 (1987).

[11] H. von Känel, Mater. Sci. Rep. **8**, 193 (1992).

[12] A. E. White, K. T. Short, R. C. Dynes, J. P. Garno, and J. M. Gibson, Appl. Phys. Lett. **50**, 95 (1987).

[13] S. Mantl, Mater. Sci. Rep. **8**, 1 (1992).

[14] N. M. Zimmerman, J. A. Liddle, A. E. White, and K. T. Short, Appl. Phys. Lett. **62**, 387 (1993).

[15] R. Jebasinski, S. Mantl, and Ch. Dieker, Mater. Sci. Eng. B **12**, 135 (1992); Thin Solid Films **223**, 298 (1993).

[16] G. Bergmann, Phys. Rev. B **29**, 6114 (1984).

[17] N. W. Ashcroft and N. D. Mermin, in *Solid State Physics,* edited by D. G. Crane (Holt, Rinehart and Winston, Philadelphia, 1981), p. 525.

[18] L. F. Mattheis and D. R. Hamann, Phys. Rev. B **37**, 10 623 (1988).

[19] B. L. Altshuler, D. Khmel'nitzkii, A. I. Larkin, and P. A. Lee, Phys. Rev. B **22**, 5142 (1980).

[20] S. Hikami, A. I. Larkin, and Y. Nagaoka, Prog. Theor. Phys. **63**, 707 (1980).

[21] S. Maekawa and H. Fukuyama, J. Phys. Soc. Jpn. **50**, 2516 (1981).

[22] A. I. Larkin, Pis'ma Zh. Eksp. Teor. Fiz. **31**, 239 (1980) [JETP Lett. **31**, 219 (1980)].

[23] B. L. Altshuler, A. G. Aronov, D. Khmelnitzkii, and A. I. Larkin, in *Quantum Theory of Solids,* edited by I. M. Lifshitz (Mir, Moscow, 1982).

[24] B. L. Altshuler, A. G. Aronov, A. I. Larkin, and D. Khmelnitzkii, Zh. Eksp. Teor. Fiz. **81**, 768 (1981) [Sov. Phys. JETP **54**, 411 (1981).

[25] W. L. McLean and T. Tsuzuki, Phys. Rev. B **18**, 503 (1984), replaced the field-independent coupling $g(T) = -[\ln(T/T_c)]^{-1}$, which enters in Larkin's $\beta(T)$ function by $g(T) = -[\ln(T/T_C) + \psi(\frac{1}{2} + DeH/2\pi k_B T) - \psi(\frac{1}{2})]^{-1}$. This agrees with the zero- and high-field limits in Ref. 26.

[26] P. Santhanam and D. E. Prober, Phys. Rev. B **29**, 3733 (1984).

[27] J. M. B. Lopes dos Santos and E. Abrahams, Phys. Rev. B **31**, 172 (1985).

[28] L. G. Aslamazov and A. L. Larkin, Phys. Lett. **26A**, 238 (1968).

[29] K. D. Usadel, Z. Phys. **227**, 260 (1969).

[30] B. L. Altshuler, A. G. Aronov, and P. A. Lee, Phys. Rev. Lett. **44**, 1288 (1980).

[31] H. Fukuyama, J. Phys. Soc. Jpn. **48**, 2169 (1980).

[32] P. A. Lee and T. V. Ramakrishnan, Phys. Rev. B **26**, 4009 (1982).

[33] G. Bergmann, Solid State Commun. **49**, 775 (1984).

[34] J. M. Vandenberg, A. E. White, R. Hull, K. T. Short, and S. M. Yalisove, J. Appl. Phys. **67**, 787 (1990).

[35] A. H. van Ommen, C. W. T. Bulle-Lieuwma, J. J. M. Ottenheim, and A. M. L. Theunissen, J. Appl. Phys. **67**, 1767 (1989).

[36] C. M. Hurd, in *The Hall Effect in Metals and Alloys,* edited by K. Mendelson and K. D. Timmerhaus (Plenum, New York, 1972).

[37] P. Santhanam, S. Wind, and D. E. Prober, Phys. Rev. B **35**, 3188 (1987).

[38] H. Fukuyama, J. Phys. Soc. Jpn. **49**, 644 (1980).

[39] H. Fukuyama, J. Phys. Soc. Jpn. **52**, 18 (1983).

[40] W. C. McGinnis and P. M. Chaikin, Phys. Rev. B **32**, 6319 (1985).

[41] In strong spin-orbit scattering material $\alpha_{ee} = g/4$, where g is the interaction constant given by $g = [1/\lambda$

$+\ln(\gamma E_F/\pi k_B T)]^{-1}$, with $\gamma=1.78$ and $\lambda=F/2$.

[42]S. Hikami, A. I. Larkin, and Y. Nagaoka, Prog. Theor. Phys. **63**, 707 (1980).

[43]G. Bergmann, Phys. Rep. **107**, 1 (1984).

[44]A. Abrikosov and L. P. Gorkov, Zh. Eksp. Teor. Fiz. **42**, 1088 (1962) [Sov. Phys. JETP **15**, 752 (1962)].

[45]B. L. Altshuler, A. G. Aronov, and D. E. Khmelnitzkii, J. Phys. C **15**, 7367 (1982).

[46]E. Abrahams, P. W. Anderson, P. A. Lee, and T. V. Ramakrishnan, Phys. Rev. B **24**, 6783 (1981).

[47]H. Fukuyama, J. Phys. Soc. Jpn. **53**, 3299 (1984).

[48]H. Fukuyama and E. Abrahams, Phys. Rev. B **27**, 5976 (1983).

[49]D. Bohm and T. Staver, Phys. Rev. **84**, 836 (1950); $c^2=\frac{1}{3}Z(m/M)v_F^2$, where m is the electron mass, M the atomic mass, Z the atomic number, and v_F the Fermi velocity.

[50]H. Takayama, Z. Phys. **263**, 329 (1973).

[51]J. C. Hensel, J. M. Phillips, J. L. Batstone, W. M. Augustyniak, and F. C. Unterwald, in *Heteroepitaxy on Silicon II,* edited by J. C. C. Fan, J. M. Phillips, and B-Y. Tsaur, MRS Symposia Proceedings No. 91 (Materials Research Society, Pittsburgh, 1987), p. 427.

[52]T. Hirano and M. Kaise, J. Appl. Phys. **68**, 627 (1990).

[53]W. R. L. Lambrecht, N. E. Christensen, and P. Blöchel, Phys. Rev. B **36**, 2493 (1987).